SolarPACES 2024, 30th International Conference on Concentrating Solar Power, Thermal, and Chemical Energy Systems

Receivers and Heat Transfer Media and Transport: Point Focus Systems

https://doi.org/10.52825/solarpaces.v3i.2453

© Authors. This work is licensed under a Creative Commons Attribution 4.0 International License

Published: 27 Nov. 2025

Opacity Measurement of Particle Curtain of Obstructed Flow Particle Heating Receivers

Rageh S. Saeed[1,2], Eldwin Djajadiwinata[1,2,*], Nader S. Saleh[1,2], Shaker Alaqel[3], Hany Al-Ansary[1,2], Brantley Mills[4], Flint Pierce[4], Abdelrahman El-Leathy[1,2,5], Syed Noman Danish[2,6], Zeyad Al-Suhaibani[1], Zeyad Almutairi[1,2,6], and Sheldon Jeter[7]

[1]Mechanical Engineering Department, King Saud University, Saudi Arabia

[2]K.A.CARE Energy Research and Innovation Center at Riyadh, Saudi Arabia

[3]Sandia National Laboratories, Mechanical Engineering, USA

[4]Sandia National Laboratories, USA

[5]Mechanical Power Engineering Dept., Helwan University, Egypt

[6]Sustainable Energy Technologies Center, King Saud University, Saudi Arabia

[7]Georgia Institute of Technology, School of Mechanical Engineering, USA

*Correspondence: Eldwin Djajadiwinata, eldwin_dj@yahoo.com

Abstract. Understanding particles flow behavior is of paramount importance in designing obstructed flow particle heating receivers (OF-PHR), and one of the important metrics is opacity of the particle curtain. In this work, the opacity is defined geometrically, i.e., ratio of area covered by the particles to the total area of the curtain. Particle curtain opacity of an OF-PHR having a single row obstruction was measured. The obstructions tested were perforated plates with two different holes-arrangements, i.e., parallel and staggered. Plate thickness, hole diameter, and pitch were measured to be 1.38, 2.84, and 4.29 mm, respectively, with angles of 60° between three adjacent holes. Two different fall distances (release point) above the obstruction were tested: 30 mm and 60 mm. The tilt angle and mass flow rate used were fixed, i.e., 0° and 1.91 kg/(s·m), respectively. The opacity was measured across a region for every 20 mm below the obstruction (0-20, 20-40, 40-60, and 60-80 mm); the opacity encompassing the whole region (0-80 mm; overall opacity) was also measured. It was found that the fall distance affects the opacity a little, i.e., doubling the distance from 30 to 60 mm only increased the opacity by 14.4% (relative change) at most. Parallel and staggered hole arrangement resulted in very close values of particle curtain opacity. Finally, it is concluded that to ensure opacity values to remain equal or greater than 85% throughout PHRs with multiple rows downstream, spacing between the perforate plate should be no greater than 40 mm.

Keywords: Opacity, Particle Curtain, Obstructed Flow, Receiver, Perforated Plate

1. Introduction

Understanding particles flow behavior is of paramount importance in designing obstructed flow particle heating receivers (OF-PHR), and one of the important metrics is opacity of the particle curtain. In this work, the opacity is defined geometrically, i.e., ratio of area covered by the particles to the total area of the curtain; it is related to the line of sight instead of the particle optical properties.

The opacity is a measure of how much sunlight directly strikes the particles, whereas the opposite of it indicates the amount reflected by the receiver base/board to the sky; therefore, it is expected that higher opacity will lead to higher receiver efficiency. Al-Ansary et al. [1] and Rageh et al. [2] conducted researches on opacity measurement using a photovoltaic sensor attached to the receiver base behind the particle curtain. The sensor measured intensity of the light that reached the back; less intensity indicated the opacity was higher and vice versa. This method, however, has drawbacks, i.e., it inherently takes into account the particle optical properties, which is the transmittivity, additional to the geometrical structure of the curtain. In fact, the sensor senses any amount of light, either direct, transmitted, or reflected, that reaches the back of the curtain (the receiver base). Another disadvantage is that it does not measure the curtain opacity in a wide area. Rather, it only measures the opacity of a small region at which the sensor is attached.

In this research, the opacity of particle curtain of receivers having a single row of obstruction was measured across a region for every 20 mm below it (0-20, 20-40, 40-60, and 60-80 mm); the opacity encompassing the whole region (0-80 mm; overall opacity) was also measured. The idea is that by knowing the opacity behavior downstream of a single row of obstruction, it can help determine the optimum distance between obstructions in PHRs having multiple rows. An optimum distance is important to avoid too low particle velocity if it is too close or excessive velocity if too far. The former will lead to (1) overheating of the obstructions and (2) extremely packed/dense particle curtain preventing sunlight to penetrate into and absorbed by the curtain throughout, whereas the latter will lead to a low opacity, causing increase in the amount of reflected sunlight to the sky.

2. Test setup

The test setup (**Figure 1** and **Figure 2**) was composed of two main parts, i.e., a particle-handling unit and PHR. The particle-handling unit was responsible for delivering particles to the PHR and then collecting the particles that left the PHR. The PHR, located just below the particle feeder, consisted of (1) a lightly white-painted acrylic board as its base and (2) an obstruction attached to the board.

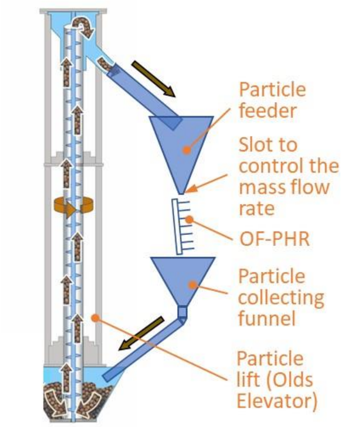

Figure 1. *Schematic diagram of the test setup at KSU.*

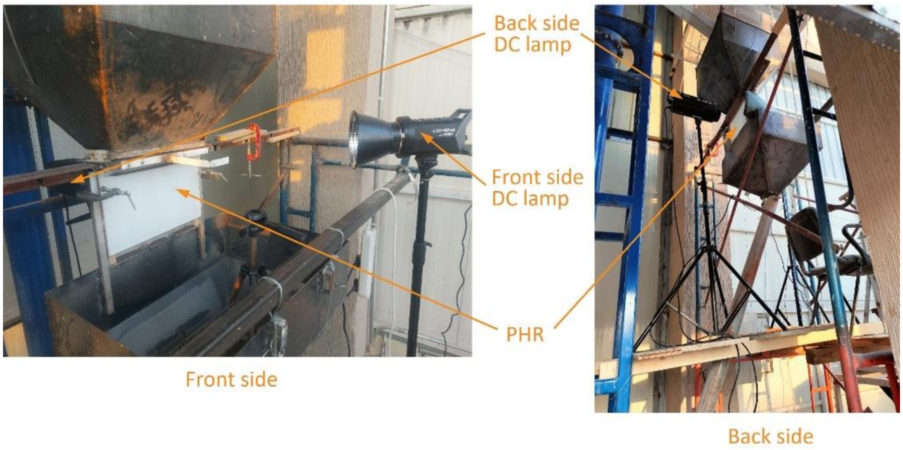

Figure 2. *Test setup along with the DC lamps, at the front and behind the PHR. These lamps are for particle velocity (not presented in this manuscript) and curtain opacity measurements.*

The acrylic board was painted white lightly to be semi-transparent (translucent); this was done to allow for good lighting during the particle-curtain opacity measurement. The tilt angle of the PHR was adjustable to allow tests at different angles; however, only tilt angle of 0° is presented here, i.e., the board is placed vertically.

The board of the PHR measured around 200 and 300 mm in height and length, respectively. It was grooved to facilitate insertion of various kind of obstructions to be tested (Figure 3 (a)). The obstruction tested was perforated plate (PP; Figure 3 (b)) installed in either (1) staggered or (2) parallel hole arrangement. These configurations were achieved by rotating the PP by 90° when cutting. The plate thickness, hole diameter, and pitch were measured to be 1.38, 2.84, and 4.29 mm, respectively, with an angle of 60° between three adjacent holes.

(a) *(b)*

Figure 3. *(a) An example of PHR from a previous project (different dimensions); (b) the obstruction tested.*

The particles used were Carbobead (CB) with an average diameter of 300 microns. To vary the particle mass flow rate, the feeder was equipped with a compartment to house an interchangeable plate with various sizes of rectangular slot; however, the mass flow rate tested in this experiment was fixed at 1.91 kg/(s·m) which corresponded with a slot size of 4.5 mm.

2.1 Particle opacity measurements

The experiments used a geometrical-based curtain opacity measurement ("line of sight") instead of the particle's material opacity. Chronos 1.4 high-speed camera was used in conjunction with a DC light. The camera is capable of recording at a maximum rate of 1069 FPS at a resolution of 1280 x 1024. The analyses were conducted using image processing software, ImageJ. An image from the videos was uploaded to the software, in which the type was changed to an 8-bit image. Thresholding was needed to divide the pixels into two regions: dark and bright, where dark represented the region covered with particles and bright was the opposite. The default auto-thresholding method in ImageJ was utilized, which is a variation of the IsoData algorithm, as stated in its manual.

A transparent acrylic board was painted white lightly to be translucent and used as the PHR base. The DC lamp was directed perpendicularly to the board from behind, and the camera was located at the front (**Error! Reference source not found.**). The paint was important to reduce the light intensity to a degree that creates good background lighting; hence, particle curtain regions that was empty from particles could be captured accurately by the high-speed camera.

(a)

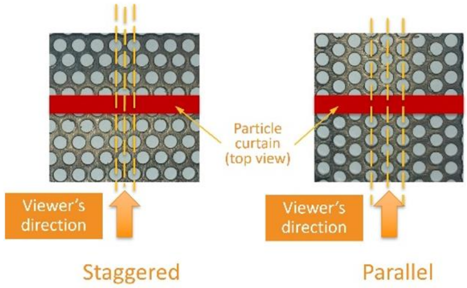

(b)

Figure 4. *The DC lamp behind the PHR (left) and the semi-transparent PHR board seen from the front (right).*

Figure 5 (left) shows some parameters used in the experiment. The distance from the tip (exit outer surface) of the particle feeder to the top surface of the obstruction, denoted as A, were 30 or 60 mm; it is referred to as falling distance or falling height. The width of obstruction, denoted as B, was 30 mm and is defined as distance from the board (PHR base) to the tip of the obstruction. The particle release distance from the board, denoted as C, was 15 mm. A summary of the varied parameters is presented in **Figure 5** (right).

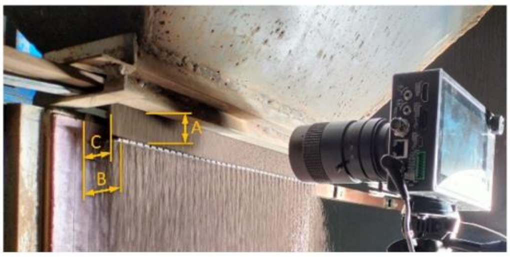

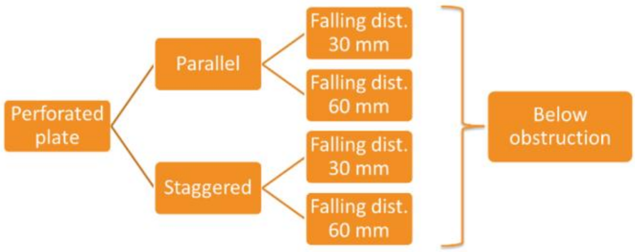

Figure 5. *Parameters used (left) and summary of the varied ones (right) for the tests.*

3. Results and discussion

3.1 Parallel hole arrangement

Curtain opacity values for PP with parallel hole arrangement were higher when the release point (falling distance) was 60 mm compared to 30 mm, i.e., 78.0% and 71.2% respectively. These opacity values were taken across a region 80 mm below the obstruction. Such a phenomenon can be attributed to (1) higher speed of particles hitting the PP for 60 mm falling distance and (2) random motion/collision of particles as they flow through the holes. These cause the particles to spread wider (back-front direction) on the obstruction, which consequently allow particles to flow through additional rows of holes of the obstruction, creating new particle layers on the curtain (**Figure 6**). Additionally, due to the random motion/collision, the projected areas of particles in the new layers do not overlap with those in the previous layers (front view projection). Therefore, these additional layers in conjunction with the effect of the particle random motion/collision increase the intercepted light. To confirm the above explanation, however, further measurement needs to be taken, such as taking videos from the side of the receiver.

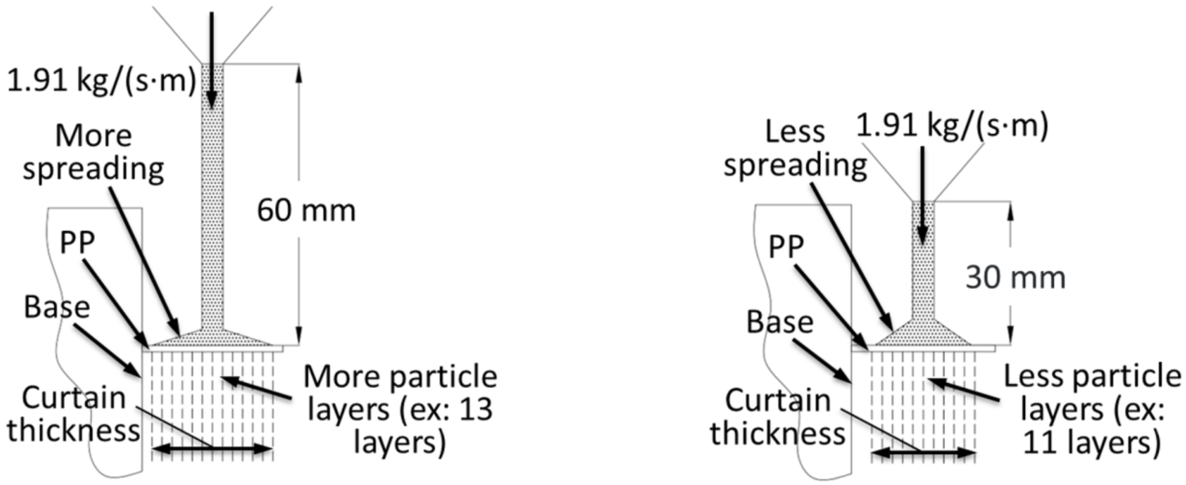

***Figure 6**. Comparison of particle spreading and number of layers in the curtain between 60 mm (left) and 30 mm (right) fall distance.*

Interestingly, although the falling distance was doubled from 30 to 60 mm, the corresponding change in opacity was only 6.8% (0.068), which was 9.6% relative to 71.2% (0.712). This implies that the obstruction effectively dissipates the kinetic energy of the impacting particles. If one relates the falling distance with velocity, assuming air viscous effect is negligible, the increase in impinging speed is $\sqrt{2}:1$ when the distance is doubled, which is equivalent to 41% increase.

A sample of the image for opacity measurement is shown in **Figure 7**; it is for the 60 mm falling distance. Note that the red region in the particle curtain image on the right does not mean it is fully empty from particles; rather, it shows a region that has low number of particles to none, which is seen by the software through the brightness (pixel value) of the pixels. The pixel values in the whole region will be taken into account by the software in calculating the opacity.

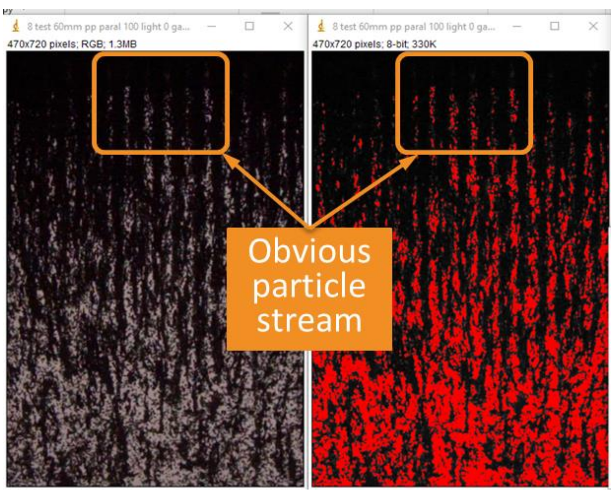

***Figure 7.** Image of opacity measurement for PP with parallel hole arrangement and 60 mm falling distance; the region covered is 80 mm below the obstruction: before (left) and after (right) post-processing by ImageJ.*

3.2 Staggered hole arrangement

Staggered hole arrangement test results show similar trend opacity values as the parallel hole arrangement. The opacity values for 30 mm and 60 mm falling distances across a region 80 mm below the obstruction are 70.0% and 80.1%, respectively, i.e, an increase of 14.4%. The reason behind it is the same as that explained in the previous section (section 3.1). **Figure 8** shows the image before and after post-processing by ImageJ; it is for the staggered hole arrangement with 60 mm falling distance.

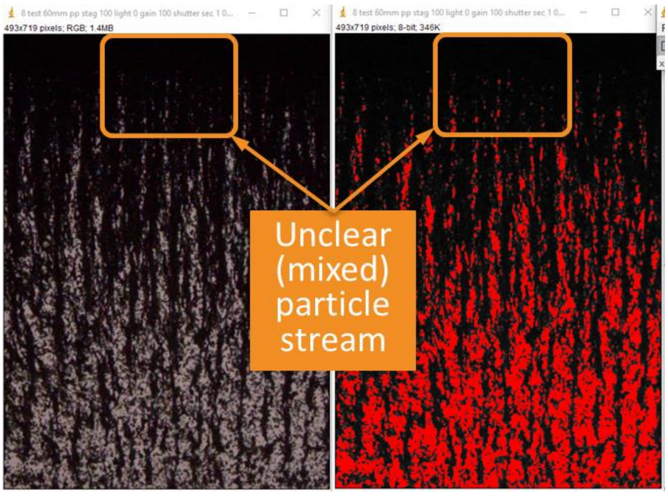

Figure 8. *Image of opacity measurement for PP with staggered hole arrangement and 60 mm falling distance; the region covered is 80 mm below the obstruction: before (left) and after (right) post-processing by ImageJ.*

It is interesting to note that despite the difference in flow pattern around the obstruction, as shown in **Figure 9**, the difference in opacity between the parallel and staggered hole arrangements, having the same fall distance/height, is small. For the parallel, the particles reach the tip, but not for the staggered. Moreover, comparing **Figure 7** and **Figure 8**, one can see that, near the obstruction, separate streams of particles are more noticeable in the parallel hole arrangement.

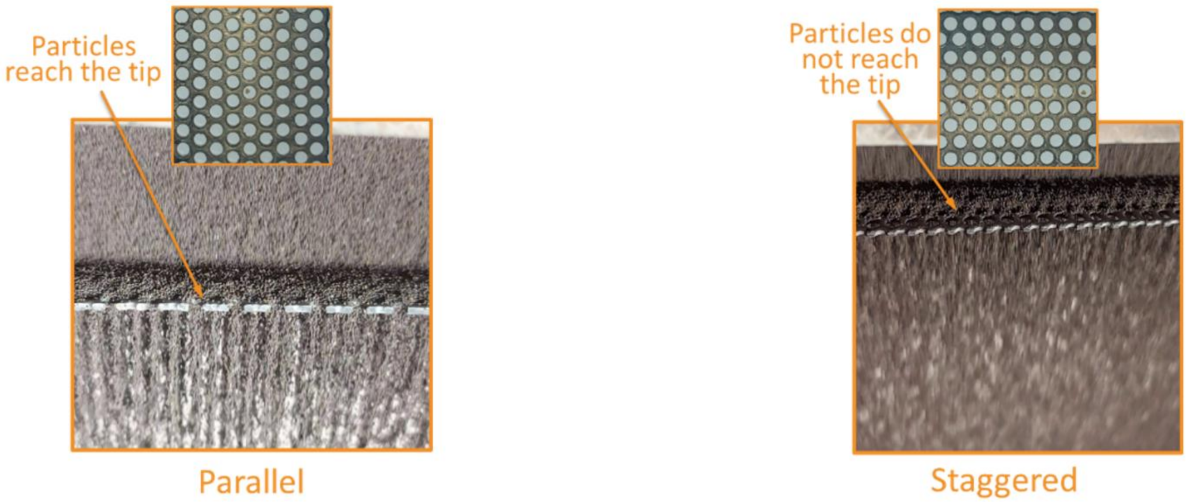

Figure 9*. Comparison of particle flow between parallel and staggered hole arrangement around the obstruction.*

3.3 Opacity for every 20 mm below the obstruction

Opacity values for every 20 mm below the obstruction are presented in **Table 1**. It shows that the opacity at every region is higher for the 60 mm fall distance than for the 30 mm, confirming the validity of the previous finding obtained from the opacity for overall 80 mm region.

Table 1. *Comparison of opacity values between parallel and staggered hole arrangement at every 20 mm below the obstruction for fall distance of 30 and 60 mm above the obstruction.*

Arrange-ment	Tilt Angle [°]	Mass Flow Rate [kg/(s·m)]	Fall dis-tance [mm]	Opacity 0-20 mm [%]	Opacity 20-40 mm [%]	Opacity 40-60 mm [%]	Opacity 60-80 mm [%]
Parallel	0	1.91	30	92.4	80.3	68.9	58.3
			60	96.2	85.8	72.5	62.7
Staggered	0	1.91	30	96.2	80.3	65.0	56.1
			60	96.9	88.1	75.8	62.9

In actual PHRs, a lot of obstructions are installed all the way from top to bottom of the board/base to increase the residence time of the particles under concentrated sunlight. To decide how far apart between obstructions should be, opacity values for every 20 mm were analyzed. The idea is that they should not be installed too far to the point where the opacity drops significantly. From **Table 1**, it can be seen that to ensure opacity values to remain equal or greater than 85% throughout the PHR, spacing between the PP obstructions should not be greater than 40 mm.

Despite this finding, further experiments with multiple rows of obstructions should be conducted to ensure its validity. Moreover, other phenomena that may affect the opacity can occur when the particles flow through these obstructions downstream, such as the tendency of particles spreading to the front, increasing the particle curtain thickness and particle spillage.

The uncertainty of the experiment was estimated by computing the root sum square (RSS) of the bias and precision uncertainties, which were 6.7% and 0.3% (absolute), respectively. The total uncertainty in the curtain opacity measurement was therefore estimated to be 6.7% (absolute) based of 95% confidence level.

4. Conclusions

Opacity measurements on a small-scale obstructed flow particle heating receiver (OF-PHR) with only a single row of obstruction has been conducted. The obstruction tested was perforated plate (PP) with two different hole arrangements, i.e., parallel and staggered. Thickness of the plate, hole diameter, and pitch were measured to be 1.38, 2.84, and 4.29 mm, respectively, with angles of 60° between three adjacent holes. The experiments were also done with two different fall distances (fall heights) above the obstruction: 30 mm and 60 mm. The tilt angle and mass flow rate were fixed, i.e., 0° and 1.91 kg/(s·m), respectively. The results are summarized as follows:

1. Higher falling distance above the PP obstruction results in higher particle curtain opacity downstream of the obstruction, which may be attributed to (1) higher speed of particles hitting the PP and (2) random motion/collision of particles as they flow through the holes. These cause the particles to spread wider (back-front direction) on the obstruction, which consequently create new particle layers in the curtain. Additionally, due to the random motion/collision, the projected areas of particles in the new layers do not overlap with those in the previous layers (front view projection). Therefore, these additional layers in

conjunction with the effect of the particle random motion/collision increase the intercepted light.

2. Despite doubling the falling distance from 30 to 60 mm, and thus, increasing the impact speed by 41%, the resulting increase in curtain opacity was quite low (9.6% for parallel and 14.4% for staggered hole arrangements). This highlights the obstruction's effectiveness in dissipating the kinetic energy of impacting particles.
3. The effect of parallel and staggered hole arrangements is not significant on the opacity of the particle curtain despite their flow pattern is rather different around the obstruction.
4. To ensure opacity values to remain equal or greater than 85% throughout the PHR, spacing between the PP obstructions should be no greater than 40 mm.

Future work will be conducting experiments on flow with multiple rows of obstructions to be able to capture particle curtain behavior on a commercial scale OF-PHR. Analyses of particle curtain thickness in relation to the opacity also need to be conducted; hence, high quality video taken from the sides of the PHR is important.

Data availability statement

The data that support the findings of this study are available from the lead and corresponding authors, Rageh Saeed and Eldwin Djajadiwinata, upon reasonable request and approval of King Saud University.

Author contributions

Conceptualization, R.S.S., E.D., N.S.S., S.A., H.A.-A., B.M., F.P., A.E.-L., S.N.D., Z.A.-S., S.J.; **Data curation**, R.S.S; **Formal analysis**, R.S.S., E.D.; **Funding acquisition**, H.A.-A., Z.A., B.M.; **Investigation**, R.S.S., E.D., B.M., F.P., N.S.S.; **Methodology**, R.S.S., E.D., B.M., F.P., N.S.S., S.A., S.J.; **Project administration**, E.D., R.S.S., B.M.; **Resources**, H.A.-A., A.E.-L., Z.A.-S., Z.A.; **Supervision**, H.A.-A., B.M., A.E.-L., S.N.D., Z.A.-S., Z.A.; **Validation**, R.S.S., E.D.; **Visualization**, R.S.S., E.D.; **Writing - Original Draft**, E.D.; **Writing - Review & Editing**, E.D., R.S.S., N.S.S.

Competing interests

The authors declare no competing interests.

Acknowledgement

The authors gratefully acknowledge the financial support provided by (1) Saudi Electricity Company (SEC), (2) King Abdullah City for Atomic and Renewable Energy (K.A.CARE), and (3) the U.S. Department of Energy Solar Energy Technologies Office through collaboration with Sandia National Laboratories, which made this work possible.

References

[1] Al-Ansary, H., El-Leathy, A., Alswaiyd, A., Alaqel, S., Saleh, N., Saeed, R., Al-Suhaibani, Z., Danish, S., Djajadiwinata, E., and Jeter, S., 2020, "Study of the Optimum Discrete Structure Configuration in Obstructed Flow Particle Heating Receivers," AIP Conference Proceedings, **2303**(1), p. 030001. https://doi.org/10.1063/5.0029145.

[2] Saeed, R., Alswaiyd, A., Saleh, N. S., Alaqel, S., Djajadiwinata, E., Al-Ansary, H., Danish, S. N., El-Leathy, A., Al-Suhaibani, Z., Almutairi, Z., and Jeter, S., 2024, "An Experimental

Investigation of Chevron-Shaped Discrete Structure Configuration on the Particle Flow Behavior of Particle Heating Receivers," Results in Engineering, **21**, p. 101786. https://doi.org/10.1016/j.rineng.2024.101786.